

## Hot Solder Dip and Minimizing Thermal Gradients

Russell T. Winslow<sup>\*a</sup>, Ganesh R. Iyer<sup>a</sup>, Minerva M. Cruz<sup>a</sup> and Guna S. Selvaduray<sup>b</sup>

<sup>a</sup>SIX SIGMA

905 Montague Expressway

Milpitas, CA 95035, USA

Ph: 408-956-0100; Fax: 408-956-0199

Email: russ@solderquik.com

\*-Corresponding Author

<sup>b</sup>Department of Chemical and Materials Engineering

San Jose State University

One Washington Square

San Jose, CA 95182-0082, USA

---

### Abstract

The semiconductor industry's move to pure-tin finishes is creating a dilemma for the high-reliability community. Most military and aerospace companies forbid the use of pure-tin because of the risk of tin whiskers. To resolve this dilemma, hot solder dip is being implemented to convert components to alternative finishes. However, poorly designed solder dip temperature profiles can induce severe thermal gradients within components, which can cause acute and/or latent defects.

This paper addresses the thermodynamic aspects of the solder dip process and provides solutions for minimizing these thermal gradients. The temperature distribution in a component was modeled using finite element analysis during three different solder dip processes. It was determined that differential temperatures were minimized when profiles with gradual preheat and gradual cool down were utilized. In addition, the model was verified by experimental results, which demonstrated a good correlation between simulated and actual measurements.

### Key words

finite element analysis, hot solder dip, thermal gradients, tin whisker mitigation

---

### Introduction

Hot solder dip (HSD) is the process of dipping the component terminations in molten solder. It is used as a final finish, and replacement finish, i.e., to change from Pb-free to Pb-bearing, or vice versa. It is also used to improve/restore the solderability of the components.

There are three types of mechanically-controlled hot solder dip: in-line style, pallet style, and robotic systems. In the in-line style, parts are clipped on a belt, which travels continuously through the soldering process. In the pallet style, a batch of parts is carried through the soldering process in a specialized fixture [1]. Robotic systems allow components to be manipulated such that only terminations are dipped into the solder.

The in-line and pallet style systems are limited to a few package styles, typically the simplest ones. In the robotic

system, the process is more flexible and hence, can accommodate almost all package types.

HSD has been used for decades as a final finish on electronic components and is currently being used as a strategy to mitigate tin whisker formation. The recent lead-free movement in the electronics industry has resulted in the use of pure tin finishes on integrated circuits and discrete components. These pure tin components bring with them the risks associated with tin whisker formation. Tin whiskers are needle-like growths that can cause electrical shorts. These minute whiskers have been linked to many failures of critical systems [2].

Hot solder dip is preferred over other tin whisker mitigation methods due to its excellent solderability protection, the complete removal of pure tin, and the ability to use any solder alloy. However, HSD does not come without potential reliability risks. Sudden and severe changes in

temperature (thermal shock) can induce delamination, warpage, broken wire bonds and/or cracks in the die. In addition, flux chemistry can become entrapped in minor delamination locations and cause corrosion, dendrite formation and/or conductive anodic filament growth. The problem is exacerbated with halogen-containing fluxes. Halogens, such as Cl, have also been reported to cause accelerated Kirkendall voiding [3].

This paper focuses on the heat transfer that occurs during hot solder dip. The temperature distribution in a 208-lead PQFP package was simulated during the hot solder dip process using finite element analysis, and experiments were conducted to verify the model.

## Hot Solder Dip

Hot solder dip typically involves five steps: (a) flux, (b) preheat, (c) solder, (d) cool down, and (e) clean. Shown in Fig. 1 is a robotic hot solder dip system [4].



Fig. 1. Robotic hot solder dip system [4].

### A. Flux

The flux performs two important functions in the solder dip process. First, it removes oxides from the solder and the surface of the components. Second, it displaces oxygen, thereby preventing re-oxidation of the surfaces [5].

### B. Preheat

Preheat serves three functions. First, it removes the volatiles from the flux. This is especially important for water-based fluxes that would otherwise cause splattering. Second, it activates the flux, and third, it minimizes thermal shock [6].

Fluxes used for solder dip become very active at elevated temperatures. However, above 150°C, most of these fluxes break down prematurely and do not function properly during the solder step.

There are several types of preheat methods, the most common of which are hot air (forced convection) and infrared. The preferred method is forced convection where heat is applied evenly to all surfaces.

### C. Solder

In the solder step, most solderable finishes (e.g., tin, gold, etc.) are replaced with the alloy composition of the solder pot.

There are two types of solder pots: dynamic and static. In the former, an oxide-free standing wave is produced by using a solder pump. In the static solder pot, some provision is made to remove the solder dross (oxides).

A solder temperature that is too low can lead to poor wetting and artifacts related to increased surface tension such as icicles, bridging, and inconsistent thickness. On the other hand, a temperature that is too high can lead to thermal damage or excessive thermal shock.

### D. Cool Down

Cool down is used to reduce the component temperature prior to clean, to prevent thermal shock. Cooling can be accomplished in several ways, either by natural convection, forced air-cooling, or a combination of both methods.

### E. Clean

Cleaning is used to remove residual flux from the component that could cause corrosion. Hot deionized water is typically utilized.

## Heat Transfer During Hot Solder Dip

During the hot solder dip process the component undergoes several rapid changes in temperature, which need to be investigated.

The immersion of the component into the molten solder is one of the most aggressive of these sudden changes in temperature. The thermal effect of exposing the component suddenly to hot solder at ~250°C is shown in Figs. 2 and 3.

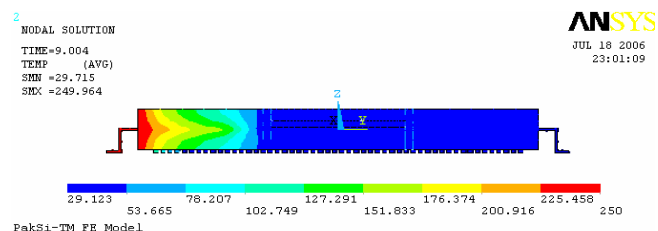
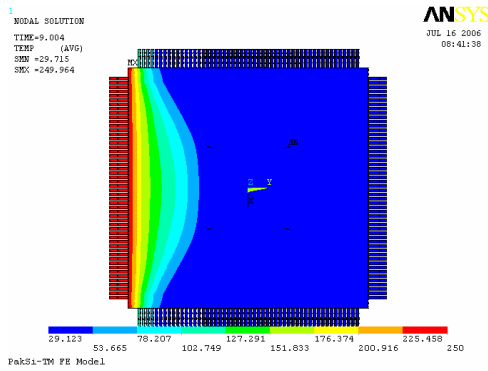


Fig. 2. Thermal simulation of a component during solder dip (cross-sectional view).



**Fig. 3. Thermal simulation of a component during solder dip (top view).**

The temperature distribution within the component can best be described using the non-steady state conduction heat transfer equation. For a semi-infinite solid, where the surface temperature is suddenly increased and maintained at temperature  $T_s$ , the non-steady state conduction heat transfer equation for temperature at any position ( $x$ ) in the solid as a function of time ( $t$ ) is:

$$\frac{\partial^2 T}{\partial x^2} = \frac{1}{\alpha} \frac{\partial T}{\partial t} \quad (1)$$

where the initial and boundary conditions are:

- (1)  $T(x, 0) = T_i$
- (2)  $T(0, t) = T_s$ , for  $t > 0$
- (3)  $T(\infty, t) = T_i$

Using the Laplace transform technique, the temperature distribution as a function of position ( $x$ ) and time ( $t$ ) can be expressed as:

$$T(x, t) = T_s + (T_i - T_s) \cdot \text{erf}\left(\frac{x}{2\sqrt{\alpha t}}\right) \quad (2)$$

where:

- $T$  is the temperature
- $T_i$  is the initial temperature
- $T_s$  is the surface temperature at  $t > 0$
- $\alpha$  is the thermal diffusivity of the material
- $x$  is the distance (position) in the  $x$ -direction
- $t$  is the time
- erf is the Gaussian error function

Thermal diffusivity is the rate at which heat is propagated through a material during changes of temperature with time [7]. It is the ratio of thermal conductivity to the product of density and specific heat capacity [8]. The higher the material's thermal diffusivity, the more rapidly it can adjust itself to the surrounding temperature.

Shown in Fig. 4 is a temperature versus time plot obtained from Equation 2, for  $x = 5$  mm. The molding compound has a much slower thermal response than copper.

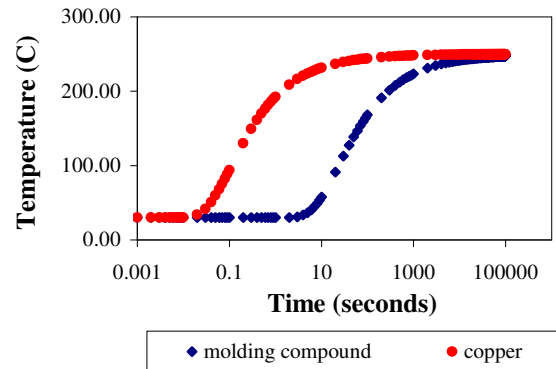


**Fig. 4. Temperature versus time plot for  $x = 5$  mm.**

## Investigation Methodology

To study the heat transfer in the component during the hot solder dip process, a two-fold study was conducted. Finite element analysis was utilized in the first part of the study to simulate the temperature distribution in the component. In the second part, experimental tests were conducted to verify the modeling. A 208-lead Plastic Quad Flat Package (PQFP) component was selected for the analysis.

### A. Finite Element Model

Finite element analysis is a simulation technique where an object is represented by a geometrically similar model consisting of finite elements. It is commonly used to find stresses, strains, displacements or temperature distributions in mechanical objects and systems.

#### 1. Description of the Model

The hot solder dip process was simulated using thermal/structural coupled-field analysis, i.e., thermal analysis followed by structural analysis. The thermal model was constructed using PakSi-TM<sup>1</sup>, transferred to ANSYS<sup>2</sup>, and then analyzed for thermal transients. The finite element model included details of the leadframe, die pad, die attach, die, and molding compound. Wire bonding effects on thermal responses were accounted for by adjusting the molding compound's thermal conductivity (between die and leads) based on the cross-section area ratio of the gold wire to the molding compound, i.e., the volume average method. In ANSYS, 8-node (SOLID 70) brick elements were used for thermal analysis.

<sup>1</sup> PakSi is a trademark of Optimal Corporation.

<sup>2</sup> ANSYS is a registered trademark of ANSYS, Inc.

## 2. Data Used for the Model

The diagram of the component and the selected data points used for the simulation are shown in Figs. 5 and 6. For the purposes of modeling, 5 points were selected for obtaining the data. Points P1, P2, P3, and P4 are 5 mm in from the edge of the component. These arbitrarily selected points provide good feedback on the temperature gradient within the component. The 5th point is at the center of the die surface, which gives the core temperature of the component.

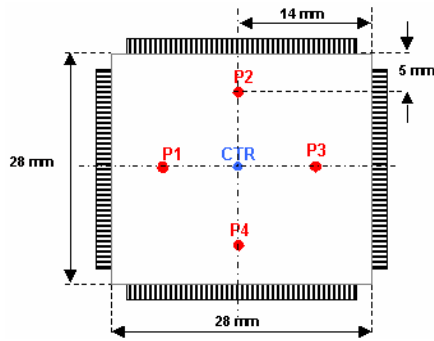


Fig. 5. Top view of the 208 PQFP with the data points used in the model.

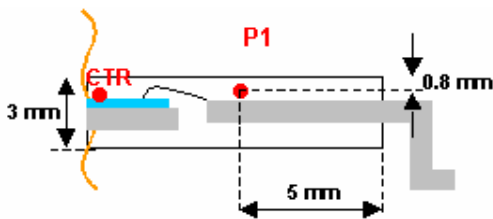


Fig. 6. Cross-sectional view of the 208 PQFP used in the model and experiment.

The properties of the materials used in the simulation are shown in Table I.

Table I  
Thermal properties of materials used in the model [9].

Material	Density (kg/m <sup>3</sup> )	Thermal Conductivity (W/m·K)	Specific Heat (J/kg·K)
Epoxy molding compound	1,820	1.05	882
Copper lead frame	8,900	301.5	385
Silicon	2,330	146	712

## 3. Test Conditions

To simulate the effects of preheat and cool down, 3 test conditions were selected:

- (1) Gradual preheat with gradual cool down
- (2) No preheat with rapid cool down
- (3) 4-sec preheat with rapid cool down

### Model Case 1: Gradual Preheat with Gradual Cool Down

This is a gradual preheat profile that helps reduce or eliminate the thermal gradient in the component. In this simulation the component was gradually pre-heated at  $\sim 3^\circ\text{C}/\text{sec}$  and gradually cooled down at  $\sim 1.5^\circ\text{C}/\text{sec}$ .

Listed in Table II are the individual steps and boundary conditions used in the model for Case 1.

Table II  
HSD process and boundary conditions used in the model for Cases 1 and 2.

Step	Temperature of Exposure	Duration (sec)	Mode of Heat Transfer
Preheat (Case 1 only)	150°C	40	Uniform forced convection heat transfer in air.
Flux	30°C	0.1	Conduction heat transfer for the edge being fluxed (leads and the edge of the package) and natural convection heat transfer (at 30°C) for the balance of the component.
Solder	250°C	3	Conduction heat transfer for the edge being solder dipped (leads and the edge of the package) and natural convection heat transfer (at 30°C) for the balance of the component.
Cool Down (Case 1 only)	30°C	15	Forced convection heat transfer in air.
Clean	60°C	10	Uniform conduction heat transfer in DI water.

The component was first preheated for 40 sec, each side was then edge dipped in flux for 0.1 sec and then soldered for 3 sec, i.e., flux, solder, flux, solder, for each side sequentially. The component was then gradually cooled using forced air for 15 sec before being immersed in DI water at 60°C.

### Model Case 2: No Preheat with Rapid Cool Down

This condition was selected to illustrate the effect of “no preheat” and “no cool down” on a component during the solder dip process. In this simulation there was no preheat and the component was quenched in DI water at 60°C. This case was identical to Case 1 except for: (a) no preheat step, and (b) no cool down step.

### Model Case 3: 4-sec Preheat with Rapid Cool Down

This condition was selected to simulate the NAVY-TMTI<sup>3</sup> robotic solder dip process [10]. In the TMTI process, all four sides of the component are edge dipped in flux, then excess flux is removed by forced air. These steps were ignored in the simulation as they are performed at room

<sup>3</sup> Transformational Manufacturing Technology Initiative

temperature and have no thermal significance. In the simulation the component was pre-heated in 150°C air for 4 seconds. After preheat, the component was solder dipped for 3 sec, one edge at a time, prior to being quenched in DI water at 60°C.

The individual steps and boundary conditions used in the model for Case 3 are listed in Table III.

**Table III**  
**HSD process and boundary conditions used in the model for Case 3.**

Step	Temperature of Exposure	Duration (sec)	Mode of Heat Transfer
Preheat	150°C	4	Uniform forced convection heat transfer in air.
Solder	245°C	3	Conduction heat transfer for the edge being solder dipped (leads and the edge of the package) and natural convection heat transfer (at 30°C) for the balance of the component.
Clean	60°C	10	Uniform conduction heat transfer in DI water.

### B. Experimental

Experimental investigations were performed to verify the accuracy of the data generated from finite element analysis. Two thermocouples were embedded in the component, as shown in Fig 6. A data logger was used to monitor and record the local temperatures during the hot solder dip process.

Points P1 and CTR correspond to those used in the FEA simulation and were selected to compare and verify the model.

Two experimental test conditions were employed:

- (1) Gradual preheat with gradual cool down
- (2) No preheat with rapid cool down

#### *Expt'l Case 1: Gradual Preheat with Gradual Cool Down*

The same conditions used in the simulation for Case 1 were used in this experiment. See Table II for details of the test conditions.

#### *Expt'l Case 2: No Preheat with Rapid Cool Down*

The same conditions used in the simulation for Case 2 were used in this experiment. See Table II for details of the test conditions.

## Results and Discussion

### A. Finite Element Model

#### *Model Case 1: Gradual Preheat with Gradual Cool Down*

In this case, the component was preheated prior to solder dip. As can be seen in Fig. 7, the component temperature reaches 135°C after 40 seconds of preheat. The temperature at P1 then drops about 10°C as the component is dipped in flux, which was at room temperature. The temperature at P1 then rises rapidly to a peak of 187°C immediately after Side 1 is dipped into the hot solder. Locations P2, P3, and P4 then follow the same trend as the 4 sides are consecutively dipped in flux then solder. During the solder dip steps, the temperature at the center of the die (CTR) decreases slightly from the preheat temperature of 135°C. This is due to cooling from natural convection and the fact that the fluxing step is repeated for each side. The temperatures at all 5 locations then converge as the component undergoes forced air cool down and clean steps.

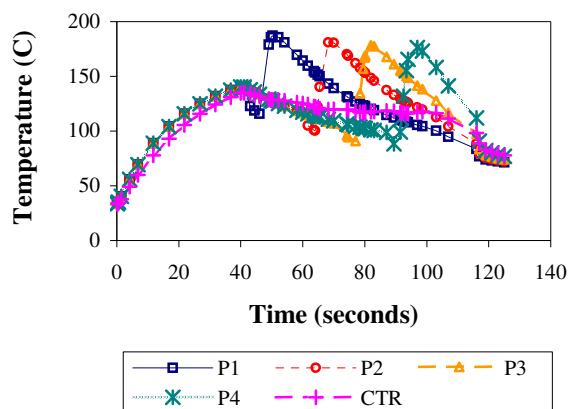


**Fig. 7. Temperature versus time plot (for Case 1).**

Shown in Fig. 8 is the difference in temperature ( $\Delta T$ ) between points P1, P2, P3, and P4 and the center of the component. This graphs also helps to locate the point in time when the temperature gradient is at a maximum. As can be seen in Fig. 8, the maximum  $\Delta T$  is 62°C and occurs immediately after each of the 4 solder dip steps.

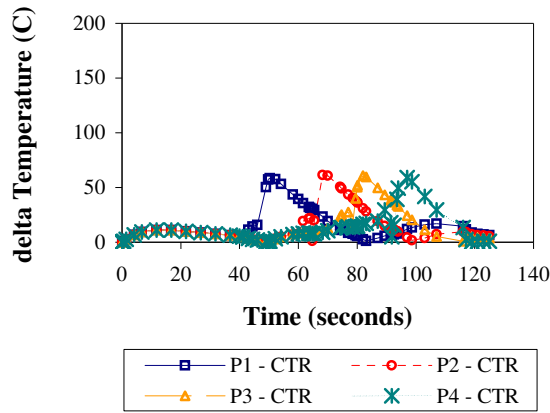


Fig. 8.  $\Delta T$  versus time plot (for Case 1).

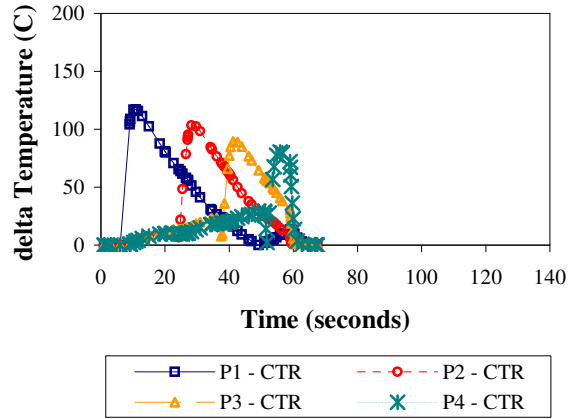


Fig. 10.  $\Delta T$  versus time plot (for Case 2).

**Model Case 2: No Preheat with Rapid Cool Down**

In this case, the component is not preheated; the temperatures at all 5 locations are at 30°C prior to the first solder step. As can be seen in Fig. 9, the temperature at P1 rises abruptly to a peak of 150°C immediately after Side 1 is dipped into the hot solder. Locations P2, P3, and P4 then follow the same trend as the 4 sides are consecutively dipped in flux then solder. During the solder dip steps the die center temperature (CTR) increases from the initial core temperature of 30°C to 84°C. This is due to the higher rate of heat transfer into the cooler (~30°C) component than in the preheated (~135°C) component from Case 1 (conduction heat transfer increases with larger differences in temperature). Immediately following the soldering of Side 4, the component is quenched in DI water at 60°C. The temperatures at all 5 locations drop sharply as soon as the component enters the water.

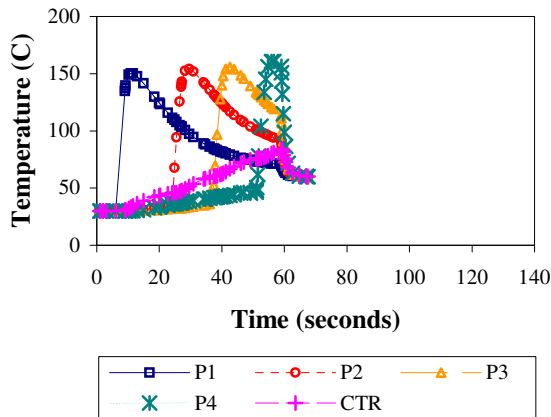


Fig. 9. Temperature versus time plot (for Case 2).

**Model Case 3: 4-sec Preheat with Rapid Cool Down**

In this case, the component was preheated for only 4 seconds; the temperatures of all 5 locations are at 52°C prior to the first solder step. As can be seen in Fig. 11, the temperature at P1 rises abruptly to a peak of 180°C a few seconds after Side 1 is dipped into the hot solder. Locations P2, P3, and P4 then follow the same trend as the 4 sides are consecutively dipped in solder. During the solder dip steps the center of the die (CTR) increases from the initial core temperature of 30°C to 109°C. This is due to the fact that more heat is conducted into the cooler package than in the preheated package, due to a larger temperature differential. In addition the solder dip steps are much closer together because the component is not fluxed between solder steps. Immediately following the soldering of Side 4 the component is quenched in D.I. water at 60°C. The temperatures at all 5 locations then drop sharply when the component enters the water.

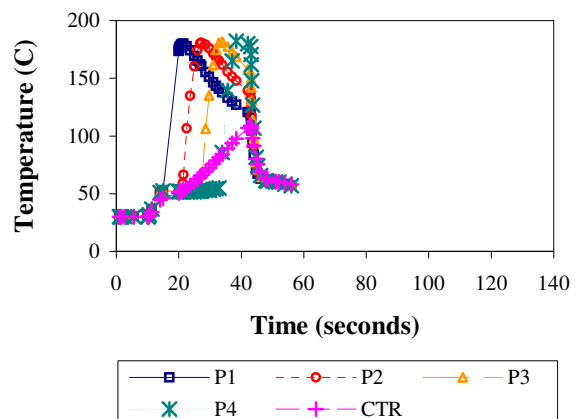


Fig. 11. Temperature versus time plot (for Case 3).

From Fig. 10, it can be seen that the maximum  $\Delta T$  is 117°C and occurs immediately after the first solder dip step. The  $\Delta T$  during the subsequent solder dip steps are not as high because the core (CTR) temperature is increasing between steps.

The maximum  $\Delta T$  is 127°C and occurs immediately after the first solder dip step, as shown in Fig. 12. The  $\Delta T$  during the subsequent solder dip steps are not as high because the

center (CTR) temperature is increasing between steps. Note that even though preheat was performed, 4 seconds is inadequate and has no impact in reducing the thermal shock on the component during solder dip.

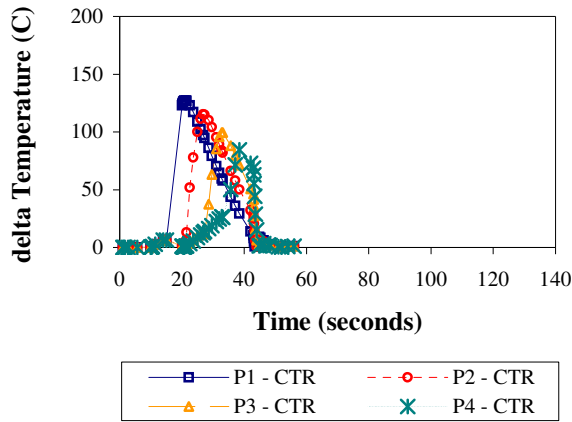


Fig. 12.  $\Delta T$  versus time plot (for Case 3).

### B. Experimental

#### Expt'l Case 1: Gradual Preheat with Gradual Cool Down

The experimental test conditions used in this case were similar to Model Case 1. In this case, point P1 reached a peak temperature of 173°C (compared to 187°C from the model) as shown in Fig. 13. There is a 4-sec shift between P1 simulated and P1 experimental, which can be attributed to timing inconsistencies between the model and the solder dip machine. In addition, the 14°C peak temperature difference may be due to minor differences in material properties, thermocouple placement, or methods of attachment.

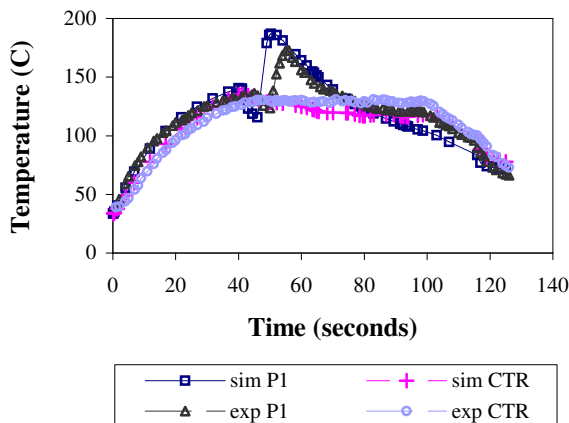


Fig. 13. Temperature versus time plot (for Case 1).

#### Expt'l Case 2: No Preheat with Rapid Cool Down

The parameters used for this case were similar to those of Model Case 2. It can be seen from Fig. 14 that point P1 has

a peak temperature of 118°C (150°C for the model). There is a 6-sec shift between the simulated and experimental P1 points, which is again due to timing inconsistencies. The rate of post solder dip cooling is slightly faster than the model. This may be attributed to the fast travel of the component in the machine, which differs from natural convection used in the model.

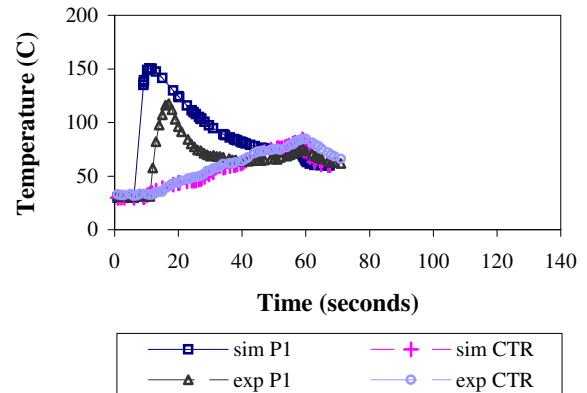


Fig. 14. Temperature versus time plot (for Case 2).

### C. Meaning and Significance of the Results

#### Advantages of Gradual Preheat

When preheat is utilized prior to solder dip, the thermal gradient ( $\Delta T$ ) in a component is reduced significantly. The results in Table IV show that components that are preheated to 135°C have a significantly lower thermal gradient than those without preheat. This is due to the lower heat flux (rate of heat transfer) from the solder into the preheated component.

Table IV  
Maximum  $\Delta T$  for each test condition.

Case	$\Delta T$ (°C)	
	Simulated	Experimental
1	62	43
2	117	77
3	127	not tested

By preheating gradually, the thermal gradient within the component during preheat is also minimized. This is important because rapidly heating the molding compound can cause the silicon die to be in tension making it particularly vulnerable to crack initiation and propagation. In fact, many component manufacturers specify a maximum rate of temperature rise between 2 and 4°C/sec during preheat prior to the reflow process [11]-[14].

#### Advantages of Gradual Cool Down

By gradually cooling the component before immersion in water, a large thermal gradient is also avoided. The cool down rates for each test case are listed in Table V.

**Table V**  
**Cool down rate for each test condition.**

Case	Simulated Cool Down Rate (°C/sec)
1	1.4
2	7.8
3	13.6

The  $\Delta T$  between the die and the component sides in the cool down step was not as obvious as those during preheat and solder dip. This is because all the data points are in the same z-direction. If one wants to determine the  $\Delta T$  during cool down, then data points must be selected along different z-positions.

## Conclusion

During the solder dip process components undergo dramatic changes in temperature. In the case of robotic solder dip the heating is typically asymmetrical. This asymmetrical heating causes severe thermal gradients within the component, which can lead to significant thermally-induced stresses. These stresses can trigger a multitude of failure modes including delamination, wire bond failure, or die cracking.

By using a combination of temperature profiling and thermal modeling these temperature gradients can be reliably predicted and measured.

Process improvements, such as properly preheating the component before solder dip and cool down prior to immersion in water, can significantly reduce these thermal gradients.

The finite element model used in this study is a valuable tool in optimizing the hot solder dip process. Now that it is proven to be accurate, it will be used as a guide to make further improvements in the process, which will minimize the reliability risks associated with hot solder dip.

Hot solder dip processes with minimal or no preheat (as in Cases 2 and 3) are not recommended as they expose the component to substantial thermal gradients.

## Acknowledgment

R. T. Winslow would like to thank Dr. Stephen Pan of TM Works for his finite element modeling contributions.

## References

- [1] Winslow Automation, Inc. Brochure. (1988). Solder Pallets for PLCC, PGA, and SOJ Packages. Winslow Automation, Inc., Milpitas, CA.
- [2] H. Leidecker and J. Brusse. (2006, Apr.). Tin Whiskers: A History of Documented Electrical System Failures. Space Shuttle Program Office, Greenbelt, MD. [Online]. Available: <http://nepp.nasa.gov/whisker/>
- [3] P. Lall, M. G. Pecht and E.B. Hakim, "Influence of Temperature on Microelectronics and System reliability," Maryland: CRC Press, LLC, p. 121.
- [4] Six Sigma Component Services. (2006). Robotic Hot Solder Dip. Six Sigma, Milpitas, CA. [Online]. Available: <http://www.sixsigmaservices.com/robotichotsolderdip.asp>
- [5] R. J. Klein Wassink, "Soldering in Electronics," 2nd ed., Scotland: Electrochemical Publications, Ltd, 1989, p. 204.
- [6] R. J. Klein Wassink, *op cit*, p. 490.
- [7] R. C. Sachdeva, "Fundamentals of Engineering Heat and Mass Transfer," New Delhi, India: New Age International, 1996, pp. 27.
- [8] R. C. Sachdeva, *op cit*, p. 27.
- [9] H.I. Rosten, J.D. Parry, J.S. Addison, R. Viswanath, M. Davies and E. Fitzgerald. (2006, May). Development, Validation and Application of a Thermal Model of a Plastic Quad Flat Pack. Flomerics. [Online]. Available: [http://www.flomerics.com/flotherm/technical\\_papers/t92/t92.jsp](http://www.flomerics.com/flotherm/technical_papers/t92/t92.jsp)
- [10] W.P. Rollins, "Partial Guideline for the Use of Robotic Solder Dipping to Replace Component Surface Finishes of Pure Tin with an Immersion Tin-Lead Finish," Navy TMTI Robotic Solder Dip Project (*unpublished draft*).
- [11] N.C. Lee, "Reflow Soldering Processes and Troubleshooting: SMT, BGA, CSP and Flip Chip Technologies," Massachusetts: Newnes Press, 2002, p. 78.
- [12] Xilinx Device Package User Guide. (2006, May). Reflow Soldering Guidelines. Xilinx Corp., Sunnyvale, CA. [Online]. Available: <http://direct.xilinx.com/bvdocs/userguides/ug112.pdf>
- [13] Intel 2000 Packaging Data Book. (2000). Board Solder Reflow Process Recommendations- Leaded SMT. Intel, Corp., Santa Clara, CA. [Online]. Available: <http://www.intel.com/design/packtech/packbook.htm>
- [14] JEDEC Standard for Moisture/Reflow Sensitivity Classification for Nonhermetic Solid State Surface Mount Devices, J-STD-020, July 2004.